9

Biomimetic Lessons Learnt from Nacre

Kalpana S. Katti, Dinesh R. Katti and Bedabibhas Mohanty
Department of Civil Engineering, North Dakota State University
USA

1. Introduction

Nacre, the inner iridescent layer of molluscan shells has been investigated for many decades due to its exceptional mechanical properties, tremendous structural redundancy and complex hierarchical structure that spans nanometer to millimeter length scale. This chapter gives an overview of past and current literature on advancements in evolution of understanding of the hierarchical microstructure of nacre, the molecular makeup of mineral and organic components, as well as recent efforts on biomimicking this structure for a variety of applications. In addition, we will also describe multiscale modeling efforts in simulating the mechanical response of this material. Modeling efforts in literature include fracture mechanics based continuum theories to molecular dynamics studies on mineral-protein interactions in nacre. The goal of this chapter would be to give the reader an in depth understanding of the existing knowledge on architecture of nacre and the structure property relationships therein. Lessons from nature to accomplish optimized mechanical response, structural redundancy and fracture toughness will be illustrated for this important material system. Also described are efforts in literature on mimicking the structure of nacre.

2. Structure and properties of nacre

2.1 Evolution

Nacre is the inner iridescent layer in many molluscan shells as shown in Figure 1. It is a type of structure which is commonly found in the molluscan classes of Gastrpoda, Bivalvia and Cephalopoda (Boggild 1930, Taylor, Kennedy and Hall 1969, Mutvei 1970, Erben 1972, Taylor, Kennedy and Hall 1973, Currey 1977). The other structural type that is found in all classes of molluscan shells has the crossed lamellar structure. Nacre is considered to be the primitive structural type and it is found in those groups that have undergone less evolutionary diversification and modification. Review of the history of various structures in bivalves can be found elsewhere (Taylor 1973). It has been reported that the organic matrix components of fossil mollusk shell is preserved for 80 million years (Weiner et al. 1979). This indicates that mollusk shells have been around for at least 80 million years. Furthermore, presence of preserved amino acids in fossil shells as old as 360 million years is reported in literature (Abelson 1954). Unfortunately, a good knowledge about the history of various structural types found in molluscan shells is not available. Most of them are made of aragonite (a crystallographic form of calcium carbonate), which is less stable than calcite.

Aragonite always tends to metamorphose into calcite with disruption of it structure (Currey 1977).

Fig. 1. Picture of a seashell showing shiny nacreous layer.

2.2. Hierarchical Structure of Nacre

Nacre exhibits a work of fracture about significantly higher than that of pure ceramic (Jackson, Vincent and Turner 1988, Jackson, Vincent and Turner 1990, Currey 1977) which is its major constituent. This is the reason why it is extensively studied in the literature for over four decades. Nacre is made up of 95% of aragonitic form of calcium carbonate ($CaCO_3$) which is a ceramic and 5% organic material primarily composed of proteins and polysaccharides. The studies in literature suggest that the main strengthening and toughening mechanisms of nacre result from its unique micro-architecture (Jackson et al. 1988, Jackson et al. 1990, Jackson et al. 1986, Wang et al. 1995, Currey 1980). Structural hierarchy is an important characteristic of all structural materials in nature such as bone, teeth and other tissues. Nacre has a very complex hierarchical microarchitecture that spans over multiple length scales from nanoscale to macroscale. At the lowest length scale, it is considered as a nanocomposite material and the microarchitecture of nacre is often described as ‘brick-and-mortar’ structure as shown in Figure 2. The bricks are made of the mineral phase and the organic matrix forms the mortar. The mineral platelets are ~5-8 μm long and ~200-500 nm thick, depending on the species and age of the shell and they are separated by layer of the organic matrix which is ~20 nm thick (Currey 1977, Jackson et al. 1988, Jackson, Vincent and Turner 1989, Jackson et al. 1990, Sarikaya et al. 1990, Currey 1980). Katti et al. (Katti et al. 2005) discovered that nacre has an “interlocked” brick-and-mortar structure with interlocking influencing the mechanical response. These platelets are mostly pseudo-hexagonal, but they may be triangular, square, or pentagonal depending on the degree of twinning on {110} planes of orthorhombic lattice (Heuer et al. 1992, Sarikaya et al. 1990). From the X-ray diffraction results, it has been found that the aragonite platelets are organized with their [001] axis perpendicular to the layers. Sarikaya (Sarikaya 1994) reported that the adjacent platelets in nacre belong to the same [001] zone axis with a slight rotation among the platelets about this axis with respect to each other. Electron diffraction revealed that there is a crystallographic relationship between the adjacent platelets, i.e. each platelet is twin-related to the platelet next to it with a twin plane of {110} type of the orthorhombic unit cell. This indicates that all the platelets on the same layer are twin-related whether they share a boundary or not. Further analysis indicated the presence of several domains with in each platelet that are crystallographically coupled. Diffraction patterns showed that two superimposed patterns can be correlated with a twin relationship with {110} twin plane parallel to [001] direction of the unit cell. Recorded patterns from all the domain boundaries showed identical twin reflections indicating that each domain is twin-related to the one next to it by a {110} twin relation.

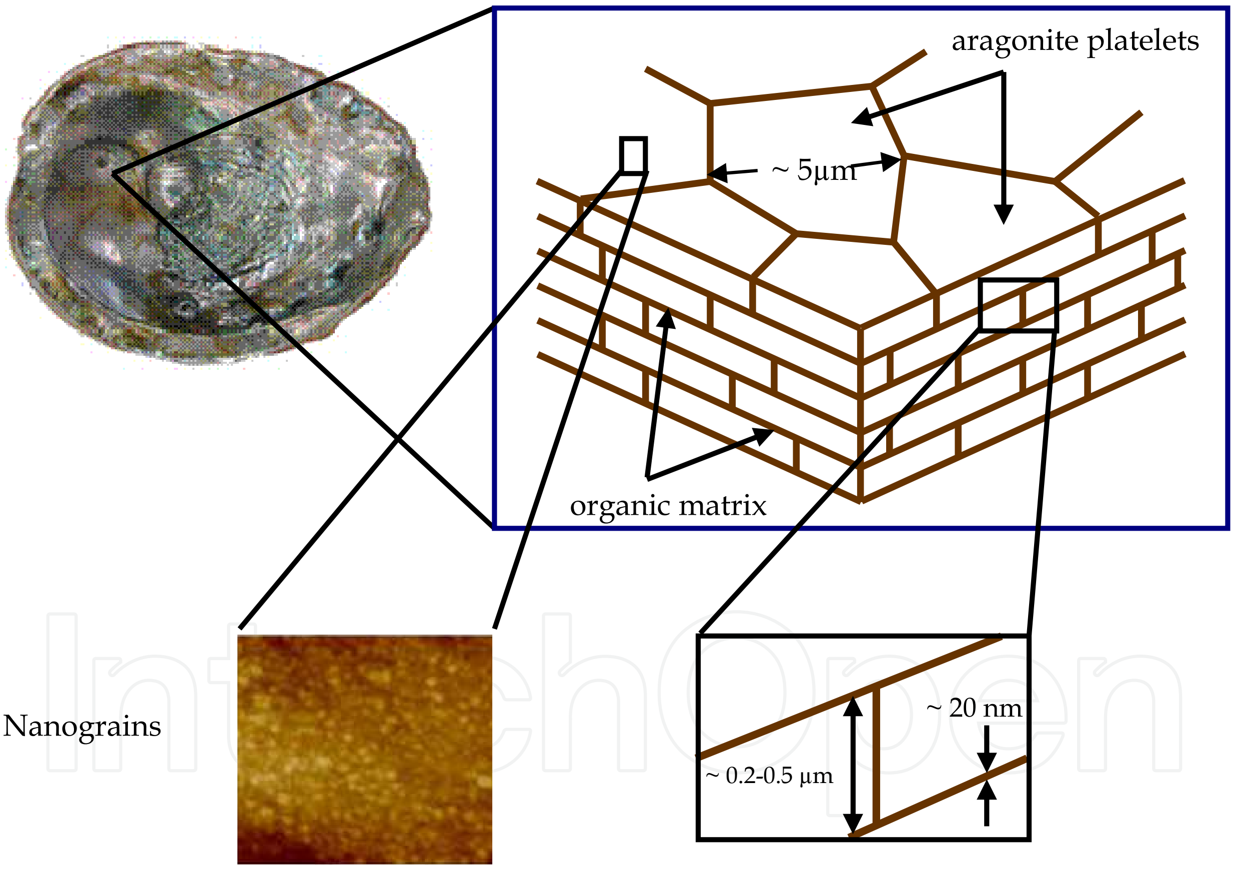

Fig. 2. Schematic representation of hierarchical structure of nacre.

Due to the large span of length scales of the hierarchical structure of nacre, various characterization methods have been utilized. Schaffer et al. (Schaffer et al. 1997) investigated the organic matrix layers of nacre by using atomic force microscope (AFM) and scanning ion conductance microscope (SICM). They observed many nanopores in the inter-lamellar organic matrix sheets. They suggested that there might be a number of mineral bridges in the organic matrix layers of nacre and proposed that the formation of nacre may be due to continuous growth of mineral bridges through these nanopores in organic matrix layers. Later Song et al. (Song, Zhang and Bai 2002, Song and Bai 2001, Song, Soh and Bai 2003) observed nacre under transmission electron microscope (TEM) and confirmed the existence of mineral bridges in the organic matrix layers. They suggested that the microarchitecture of nacre should be considered as "brick-bridge-mortar" structure rather than the traditional "brick and mortar" arrangement. Based on their observation, they proposed a distribution law of mineral bridges in the organic matrix layers using statistical methods. These mineral bridges were circular in shape with a diameter of ~25-34 nm and the height being equal to the thickness of organic matrix. Density of the mineral bridges was estimated to be approximately 91-116 μm^{-2}. Nanoscale mineral island-like structures were observed using atomic force microscopy (AFM) and scanning electron microscopy (SEM) (Wang et al. 2001, Evans et al. 2001). These were called as nanoasperities and were about 30-100 nm in diameter, 10 nm in amplitude, and separated 60-120 nm. Later, Kattis and co-workers (Katti et al. 2005) discovered the presence of interlocking between the platelets of nacre. The mineral platelets are rotated by a small angle relative to each other and form the interlocks by interpenetrating into each other. Scanning electron microscopy imaging of fractured surface of nacre first revealed the presence of extensive interlocking in nacre as shown in Figure 3. They showed that the bricks are not only stacked upon one another to form a brick wall but also interpenetrated into one another to form interlocks. Further, Li et al. (Li et al. 2004) observed that the aragonite platelets consist of polygonal nanograins which are the basic building blocks in nacre. Observation of screw dislocations in nacre has been reported as early as the 1950s in literature (Watabe 1955). Wise et al. (Wise and Devillie.J 1971) showed the significance of these screw dislocations in the crystal growth of the aragonite platelets. Yao et al. (Yao, Epstein and Akey 2006) confirmed the presence of these screw dislocations by excavating individual aragonite platelets using a nanomanipulator with in-situ SEM/FIB. They suggested that the crystal growth in nacre occurs via spiral motion which is responsible for the identical crystal orientation in the successive layers. Nacre contains 106 screw dislocations per square centimeter which is three orders of magnitude higher as compared to typical ionic or covalent crystals. Thus the architecture of nacre spans from molecular, nanograin, defect structures of crystals, mineral bridges, asperities, polygonal, interlocked bricks over the atomic to 10s of microns of length scale with strengthening and toughening mechanisms associated with each length scale.

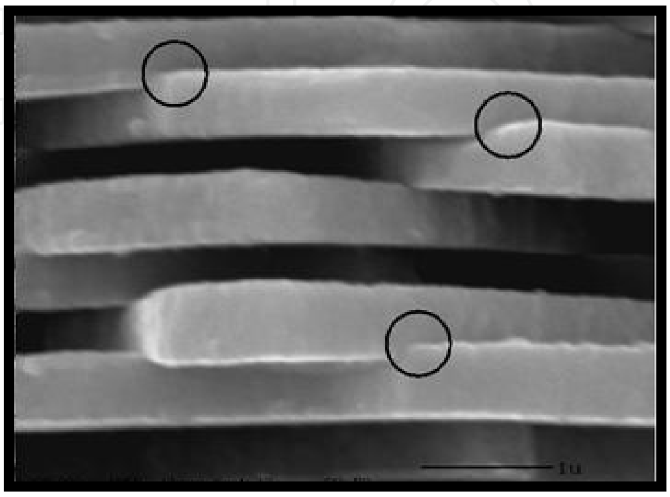

Fig. 3. SEM of nacre showing interlocks (Katti et al. 2005).

2.3. Molecular Structure

Although the molecular structures of components of nacre: the mineral platelets and organic mortar are known to have very significant role on its mechanics, far lesser studies have been conducted on evaluation of molecular structures as compared to the architectures. Weiner and co-workers (Weiner 1979, Weiner and Traub 1980, Weiner and Traub 1981, Weiner, Talmon and Traub 1983, Weiner 1983, Weiner and Traub 1984, Weiner 1984, Addadi and Weiner 1985, Addadi et al. 1987, Addadi and Weiner 1997, Nudelman et al. 2006), as well as Morse and co-workers (Fritz et al. 1994, Zaremba et al. 1995, Zaremba et al. 1996, Schaffer et al. 1997, Shen et al. 1997, Smith et al. 1999, Belcher et al. 1996, Su et al. 2002) have made significant efforts in understanding the organic matrix and biomineralization in molluscan shells. The organic matrix in nacre primarily consists of proteins, with some glycoproteins and chitin. Different proteins play different roles such as: some provide nucleation sites for the growth of aragonite crystals, some are responsible for the secretion of calcium carbonate, and many of them help in stabilizing the aragonite crystal arrangement. Presence of β-sheet structures in an antiparallel conformation was indicated by the infrared spectroscopic results and the amino acid compositions of insoluble shell matrices resembled those of silk fibroins in their content of glycine, alanine and serine, which together constitute more than 50% of the total (Weiner and Traub 1980). The silk-fibroin like protein, in some cases associated with chitin may contribute to the structural basis for the elaboration of the organic matrix framework around which the mineral is deposited. X-ray diffraction studies revealed a well defined spatial relationship between orientations of the protein, chitin and aragonite. The a-axis of the aragonite orthorhombic cell is lined up with the b-axis of chitin and the b- and c- axes of the aragonite lie along the b- and c- axes of the protein respectively. The identification of proteins present in the organic matrix has only been partially done to this date. Although researchers have succeeded in extracting protein from the shells and causing precipitation from the supersaturated solutions of Ca^{2+} and CO_3^{2-} (Addadi and Weiner 1985). Weiner and co-workers (Addadi and Weiner 1985, Weiner and Traub 1980, Addadi et al. 1987) have suggested the presence of aspartic acid-rich proteins (Asp-Y)n, and serine-rich proteins, where Y is an amino acid. The aspartic acid-rich proteins have amino acid composition: Aspartic acid, 32%; Serine, 10%; Glutamic acid, 17%; Glycine, 7% and are often associated with small amounts of polysaccharides. The serine-rich proteins have a amino acid composition: Aspartic acid, 7%; Serine, 25%; Glutamic acid, 8%; Glycine, 19%. Constituents of both these proteins bind to Ca^{2+} and undergo conformational changes. It is believed that the aspartic acid-rich proteins adopt the β-sheet conformation (Addadi and Weiner 1985). The phenomenon of stereo-selectivity has been described in considerable detail and three possible reasons have been suggested: (1) The aspartic acid rich proteins bind preferentially to the calcium atoms, (2) A favorable electric charge is created on the (001) face for the protein adsorption due to the relative position of calcium and carbonate ions, and (3) The coordination around the protein-bound calcium atoms are completed as the carboxylate groups (CO_3^-) are oriented perpendicular to the (001) face. It has been further proposed that the aspartic acid-rich domains are covalently bonded to sulfated polysaccharides, and these sulfates cooperate with β-sheet structured carboxylates for oriented calcite crystal nucleation (Addadi et al. 1987). The sulfates help concentrate calcium, creating the super-saturation required for nucleation on the structured carboxylate domains. The basis of cooperative mechanism is attributed to the distinct ways in which carboxylates and the sulfates interact with calcium ions. The sulfates are strongly associated with calcium, and carboxylates are relatively weak binders of calcium. Carboxylates being a part of an ordered protein structure help in binding calcium ions in an ordered array.

Morse and co-workers investigated the biomineralization process in red abalone shells by inserting different materials including flat pearls as substrates between the mantle and shell (Fritz et al. 1994, Belcher et al. 1996, Zaremba et al. 1996). Exposure of mantle epithelial cells to a foreign material causes the secretion of proteins that activate growth of calcite layer with preferred {104} orientation, which is followed by the growth of nacreous aragonite. The transition from {104} oriented calcite growth to aragonite growth is abrupt. It is suggested that the formation of mineral structure and the molluscan shell architecture are controlled by the interaction at the cell-mineral interface. Belcher et al. performed in vitro crystallization of calcium carbonate in the presence of water-soluble polyanionic proteins extracted from abalone shell. It was found that these proteins are sufficient to control the crystal phase and govern the transition between calcite and aragonite growth. These proteins are also necessary for the control of nucleation and crystal orientation. Shen et al. characterized the cDNA coding for Lustrin A, which is a protein they identified and is present in the organic matrix in the nacreous layer of red abalone (Shen et al. 1997). Analysis of amino acid sequence of this protein revealed that it exhibits a highly modular structure with a high proportions of Serine (16%), Proline (14%), Glycine (13%) and Cystine (9%). It contains ten cystine-rich domains (C1-C10) and eight proline-rich domains (P1-P8). These praline-rich domains are present between the cystine-rich domains and act as extenders allowing them to work independently. The gylcine- and serine-rich domains lie between the cystine-rich domains near the C terminus. It was shown that the mineralization of nacre is controlled by the cystine-rich domain, and the proline-rich domains act as spacers between the cystine domains. Further, Lustrin A is multifunctional protein that combines several structural elements into a single molecule. Su et al. (Su et al. 2002) characterized the growth lines in red abalone shell using X-ray diffraction, and scanning and transmission electron microscopy. The growth lines were observed to consist of two types of structures: blocklike and spherulitic, separated by a green organic matrix interlayer. Both these structures are composed of aragonite, the same $CaCO_3$ polymorph as in the nacreous layer. The spherulitic structure is composed of radially distributed elongated crystals and the block-like structure is made up of crystalline aggregates with irregular shape. The size of the individual aggregates is similar to that of a single crystal and the orientation is identical to that of the adjacent stack of tablets in the nacreous structure. Nudelman et al. (Nudelman et al. 2006) mapped the distribution of organic matrix components underlying a single aragonite platelet in nacre. Four different zones were observed under a single aragonite platelet: a central spot rich in carboxylates which is surrounded by a ring-shaped area rich in sulfates, third zone is the area between the central nucleation region and the imprint periphery containing carboxylates, and the fourth zone is the intertabular matrix which is rich in carboxylates and sulfates. Gilbert et al. (Gilbert et al. 2008) investigated red abalone shells using X-ray photoelectron emission spectromicroscopy and suggested that orientational ordering of aragonite tablets in nacre do not occur abruptly but gradually over a distance of 50 μm from the prismatic boundary. They suggested that different crystal orientations in nacre tablets correspond to different growth rates. All the tablets try to grow and compete for space. The oriented tablets grow faster than the misoriented ones and create ordering in nacre. It was also suggested that the ordering of the mineral phase may be independent of biological or organic-molecule control.

Kattis and co-workers have performed FT-IR (Fourier transform infrared) spectroscopic experiments (Verma, Katti and Katti 2006, Verma, Katti and Katti 2007) and molecular dynamics (MD) simulations (Ghosh, Katti and Katti 2007, Ghosh, Katti and Katti 2008) to understand the organic-inorganic interactions in nacre at molecular level. Verma et al. (Verma et al. 2006) performed PA-FTIR (photoacoustics FTIR) experiments on undisturbed nacre as well as powdered nacre and compared the results. The observed differences in PA-FTIR spectra of nacre powder and undisturbed nacre are believed to arise from two sources: breaking of bonds between organic and inorganic phases, and relaxation of residual stress that exists in the structure of nacre. They also investigated the stratification in nacre using PA-FTIR experiments in step-scan mode. Results did not indicate any significant compositional changes in the mineral and protein layers. In another study, Kattis and coworkers (Verma et al. 2007) performed 2D-FTIR spectroscopy and deconvolution analysis to investigate the nature and location of water present in nacre. They found three different forms of water present at various locations in nacre as shown in Figure 4. One of the forms is partially hydrogen bonded possibly hydrogen bonded with the organic matrix. Second form of water is fully hydrogen bonded with the surrounding water molecules and is similar to bulk water. This form of water is possibly located in the pores of the organic matrix and the organic platelets. Third form of water is the chemisorbed water present on the surface of the aragonite platelets. Polarization experiments indicated that the water present in nacre exhibits a preferred orientation. The H-O-H plane of water molecule is oriented parallel to the c-axis of aragonite platelets. Furthermore, molecular models of organic and mineral phase were built and steered molecular dynamics simulations were performed to understand the effect of mineral-protein interaction in the work of Kattis and co-workers (Ghosh et al. 2007). In this work, glycine-serine domain of a nacre protein Lustrin A was used as a model system. The protein molecule was pulled in absence and presence of mineral phase as shown in Figure 5. Obtained load-displacement curves indicated that the mechanical response of the organic phase in nacre is significantly influenced by the mineral proximity. It was observed that the energy required to pull the protein molecule in the proximity of mineral is several times higher than when the mineral is absent. Further, the pulling velocity of the protein molecule influences the factor by which additional amount of energy is required to unfold a protein domain. In another study, Kattis and co-workers (Ghosh et al. 2008) quantitatively described the specific mechanisms responsible for the differences in load-displacement (L-D) responses of protein at mineral proximity and absence of mineral. It was shown that the peaks in the L-D plot can be directly correlated to the interaction energies between the atoms involved in the latching phenomenon of amino acid side chain to aragonite surface during the early stage of pulling. Further, water plays a significant role in the mineral-protein interaction. Water close to the mineral phase is highly oriented and does not move while the protein is being pulled. The layer of water around the protein strands moves with the strand as the protein is pulled. Attractive interactions between the various constituents, the protein, protein-bound water, and the mineral are primarily responsible for the high magnitude of load required for a given displacement. These studies indicate a significant role of organic-inorganic interactions in the mechanical response of nacre and the important role of water in these interactions.

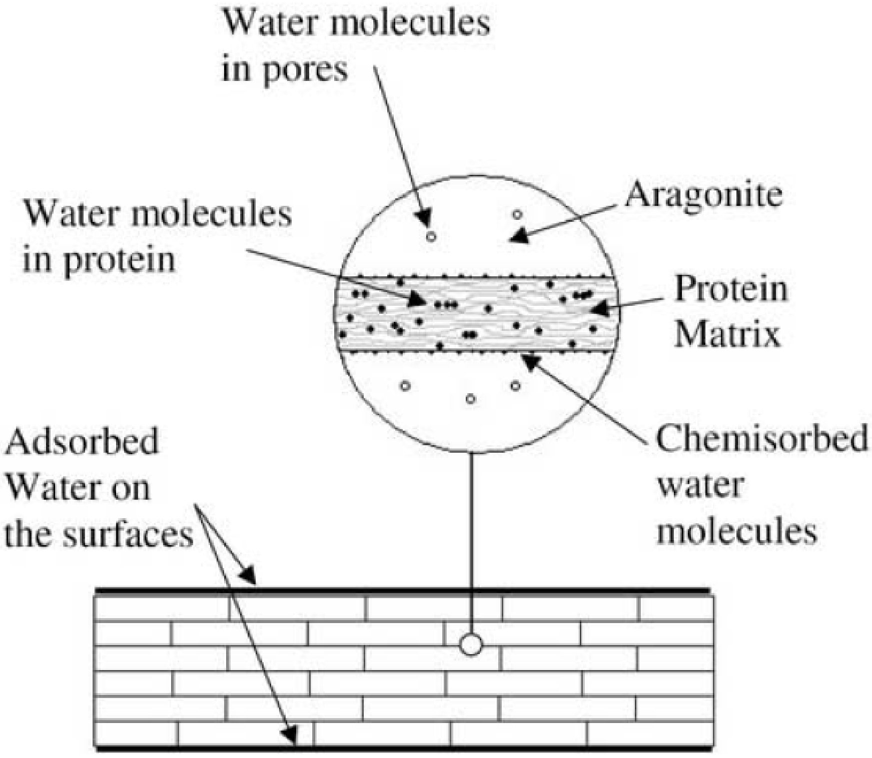

Fig. 4. Schematic showing presence of water clusters in the protein matrix and chemisorbed water molecules at the interface (Verma et al. 2007)

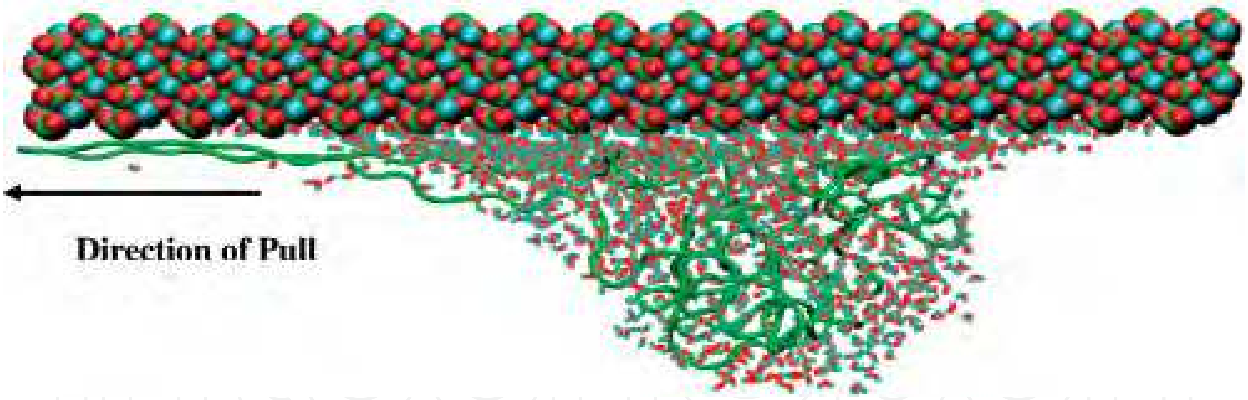

Fig. 5. Model of Glycine – Serine (GS) domain at mineral proximity as the GS domain is pulled. The ball form with the cyan, red, and green combination is atoms in aragonite, the ribbon form in green is the GS domain, and the line form with red and cyan lines represents water (Ghosh et al. 2007).

2.4. Mechanical properties

Literature shows several comparative studies on the mechanical properties of various structural types found in molluscan shells (Taylor and Layman 1972, Currey and Taylor 1974, Currey 1976). It is clear that nacre is stronger than other structures irrespective of the loading type. The extraordinary toughness possessed by nacre was first described by Currey

(Currey 1977). He suggested that the mechanical properties of nacre result from its structure and specifically, the highly organized micro-architecture with precise arrangement of mineral platelets. This arrangement of mineral platelets obstructs crack propagation. Later, Jackson et al. (Jackson et al. 1988) performed an extensive experimental study on the mechanical properties of nacre and tested nacre in dry and wet conditions. They reported Young's moduli values of 70 GPa and 60 GPa for dry and wet samples respectively. The tensile strength of nacre was found to be 170 MPa for dry and 140 MPa for wet samples. Depending on the span-to-depth (S/D) ratio and degree of hydration, the work of fracture varied between 350 to 1240 J/m^2. In contrast, the observed work of fracture for monolithic $CaCO_3$ was about 3000 times less than that of nacre. They found that the water absorbed in the organic matrix of nacre plays a significant role in the mechanical response of nacre. Presence of water reduces the Young's modulus and tensile strength, where as the work of fracture shows pronounced increment. Nacre exhibits a work of fracture which is almost three times when wet as compared to dry nacre. Water may cause reduction in shear modulus and shear strength of the organic matrix which in turn reduces the Young's modulus and tensile strength. Significant improvement in the toughness might be due to the plasticizing of organic matrix by water. This plasticizing of the organic matrix may cause debonding around the crack tip. They also pointed out that the nacre platelets have small S/D ratios making them more ductile and there by increasing the ability to absorb more energy. In another study Jackson et al. (Jackson et al. 1990) compared the properties of nacre with different synthetic composites that had high volume percent of ceramic phase and a minor organic phase as the matrix. The closely packed layered structure and soft organic matrix were the two features that distinguished nacre from other synthetic composites used in the study. Further, they found that nacre is stiffer, stronger and tougher than the synthetic composites. After these key studies by Currey and Jackson et al., literature was deluged with various kinds of studies involving experiments and modeling to understand the mechanisms responsible for the high toughness in nacre. Various experimental techniques have been used to understand the mechanical behavior of nacre at different length scales and their relationship to the microstructure. Modeling techniques such as finite element analysis (FEA) and molecular dynamics (MD) have been used to get an insight into the mechanisms enhancing the mechanical behavior of nacre.

Experimental evaluation using fractographic and ultramicrostructural analysis using scanning electron microscopy (SEM) and transmission electron microscopy respectively have also been conducted (Sarikaya et al. 1990). conducted mechanical tests on nacre samples. Similar tests were also carried out on alumina and partially stabilized zirconia samples for comparison. From the indentation experiments it was observed that cracks extend radially from the corners of the indentation in case of the pure ceramic samples, indicating brittle behavior. Similar tests on transverse direction in nacre indicated that cracks do not extend from corners of the indentation, but from regions close to corners and propagate in various directions. They suggested that these directions might be the high strain regions formed due to the complex stress distribution in the nacre structure. The path of the cracks and microcracks were very tortuous which indicated a large amount of energy absorption in the form of deformation during the crack propagation. This resulted in higher fracture toughness as compared to other monolithic ceramics. From the fractographic analysis of the fracture surfaces and indentation cracks, they suggested several possible mechanisms for toughening of nacre. These mechanisms are crack blunting/branching, microcrack formation, platelet pull-outs, crack bridging (ligament formation), and sliding of layers. They concluded that all these mechanisms have to be operative in nacre to increase the fracture toughness and strength. High tortuousity seen in the crack propagation was mainly due to crack blunting and branching, and the totuousity was not considered the major toughening mechanism. Wang et al. (Wang et al. 1995) used SEM, TEM and microindentation tests to study the deformation, fracture and toughening mechanisms in nacre. Their results revealed anisotropic nature in fracture and microindentation morphologies, as well as the cracking behavior of nacre. And this reflects the microstructural character of nacre. It was observed that the fracture surface parallel to the cross-sectional surface is much more tortuous as compared to the surface that is parallel to the platelet surface. Step-like crack lines were seen on the cross-sectional surface where as it is polygonal on the platelet surface. They suggested that the major plastic deformation mechanism in nacre is the sliding of the aragonite layers combined with plastic deformation in the organic matrix. They concluded that there are three major toughening mechanisms in nacre acting simultaneously: crack deflection, fiber pull-out, and organic matrix bridging. Smith et al. (Smith et al. 1999) pulled the organic molecules from a freshly cleaved nacre surface using atomic force microscope (AFM) and obtained consecutive force-extension curves without touching the surface between the pulls. They observed rupture events with a saw-tooth appearance in each of the obtained force-extension curves. Observed hysteresis after completion of a pulling cycle demonstrated that work has been done on the shell which is irreversible and is dissipated in the form of heat. The dissipated heat was found from the area between the retracting and approaching parts of the curve, and it was found to be of the order of (0.4-1) x 10^{-17} J per cycle. Each peak in saw-tooth curve indicates opening of intra-chain loops or folded domains within a single molecule. This may also indicate the successive release of sacrificial inter-chain bonds crosslinking multiple chains together in the matrix. They concluded that breaking of sacrificial inter-chain bonds and opening of folded domains absorb energy and contribute towards the high toughness of nacre. Song et al. (Song et al. 2002, Song and Bai 2001, Song et al. 2003) observed the presence of mineral bridges using TEM. To investigate the effect of mineral bridges, they performed tension and three-point bend tests on dry nacre samples and examined the fracture surface morphology. They found that the organic matrix layer is linear elastic in the direction of mineral bridges and undergoes very small deformation before crack extension. All the cracks were observed to propagate through the organic matrix layers. They suggested that the presence of mineral bridges significantly affects the organic matrix layers by enhancing the stiffness, strength and toughness. Mineral bridges in organic matrix layers are intimately associated with the two major toughening mechanisms in nacre: crack deflection and platelet pull-out, because of the unique microstructure of nacre. They concluded that nacre possesses a high toughness because of the existence of mineral bridges in the weak layers where as other synthetic materials with “brick and mortar” structure do not have a toughness comparable to nacre. It has been discussed in the previous section that nanoasperities were observed on the surface of platelets in nacre (Wang et al. 2001, Evans et al. 2001). Wang et al. (Wang et al. 2001) and Evans et al. (Evans et al. 2001) showed that deformation in nacre is inelastic both in shear and tension. And the nanoasperities on the surface of aragonite platelets govern the stress at which the inelastic deformation proceeds. The interposing arrangements of nanoasperities control the sliding resistance that facilitates the observed ductility in nacre. They suggested that the organic matrix and nanoasperities play a key role in toughening of nacre. Based on their study, they identified four design principles that impart high toughness to nacre. (i) The mineral phase possesses tabular morphology and is optimized with plate size, aspect ratio, and topological arrangements to maximize the inelastic strain. (ii) The amplitudes and wavelengths of nanoscale asperities on the platelet surface cause strain hardening large enough to form multiple dilatation bands, but not so large which may lead to internal fracture of the platelets. (iii) Organic interlayer has sufficient adherence and transverse stretch that keeps the platelets intact in the regions between dilatation bands, where transverse tensile strains are generated. (iv) Organic matrix provides high lubrication that makes the interface slip frictionless. Meyers and co-workers studied the quasi-static as well as dynamic mechanical response of Haliotis rufescens (abalone) (Menig et al. 2000) and Strombus gigas (Menig et al. 2001) (conch) shells. From their observations, they suggested that the shell structure imparts a significant increase in the toughness of the brittle aragonite mineral. They identified two primary toughening mechanisms in nacre: (i) sliding of mineral platelets by means of viscoplastic deformation of the organic interfacial layers; (ii) arrest and deflection of cracks by the viscoplastic organic layers. These two mechanisms and the highly organized microstructure, consisting of mineral platelets, lead to delocalization of failure. Due to this delocalization of failure, one single sharp crack is replaced by a large number of smaller cracks in a broader region. Kamat et al. (Kamat et al. 2000) indicated that the cracks do not propagate catastrophically through the middle layers of mollusk shells and the crack propagation retarded by the bridging action of the first-order lamellae.

Kotha et al. (Kotha, Li and Guzelsu 2001) modeled the tensile behavior of nacre using a modified shear lag theory. They used a two-dimensional model to analyze the stress transfer between the aragonite platelets. They suggested that composites having high toughness can be made using platelets with small aspect ratios, but the matrix should be designed to have high shear strains. Organic matrix can have high shear strains through the presence of loops or domains that break at different strains.

Katti et al. (Katti et al. 2001, Katti and Katti 2001, Katti, Pradhan and Katti 2004, Katti et al. 2005) studied the mechanical response of nacre using finite element modeling and experimental techniques to understand underlying mechanisms responsible for the high toughness of nacre. Their results led to important findings that give a better insight about the mechanical behavior of nacre. 3D finite element modeling results indicated that a very high (400 MPa) yield stress of the organic phase is needed to obtain the stress-strain behavior and yield stress of nacre observed experimentally (Katti et al. 2001). This value of yield stress is higher than the observed values for real proteins and biological tissues. Necessity of the high yield stress is due to higher effective local stresses in organic phase than applied. They suggested that the organic phase might be a composite containing a high yield stress component. Also, high yield stress of the organic phase may be due to the presence of possible hard contacts between the mineral platelets through the organic layer causing higher stress in organic phase than applied. In another study using finite element simulations, Katti et al. (Katti and Katti 2001) showed that the organic phase possesses an elastic modulus of ~15 GPa. This value of elastic modulus is higher than the reported values for the organic phase by three orders of magnitude. Katti et al. (Katti et al. 2004) evaluated the role of nanoscale asperities present on the aragonite platelet surface. These nanoasperities were incorporated in the finite element models as shown in Figure 6 and simulations were performed using different values for the yield stress of the organic. The results revealed that the nanoasperities have a marginal effect on the over all mechanical response of nacre. In the elastic regime, a small increase in elastic modulus was observed due to the presence of nanoasperities, part of which resulted because of increase in mineral volume and part due to the structural effect of nanoasperities. No significant effect of nanoasperities was observed in the inelastic regime. As discussed in the previous section, Katti et al. (Katti et al. 2005) discovered the presence of platelet interlocks in the structure of nacre. They also evaluated the effect of these interlocking features on the mechanical behavior of nacre by incorporating them into finite element models as shown in Figure 7. Finite element analysis results revealed that these platelet interlocks play a key role in imparting high toughness and strength to nacre. Interlocks function as physical obstacles to the relative movement of the mineral platelets. Thus, these interlocks must break before the load is completely transferred to the organic matrix. Further, these interlocking features might play a role in inhibiting crack propagation by crack branching and blunting. Platelet interlocks are spread throughout the volume of nacre and collective influence of these interlocks from different layers is translated into the bulk mechanical response of nacre. This results in a significant enhancement of fracture toughness and strength by providing a mechanism for energy dissipation.

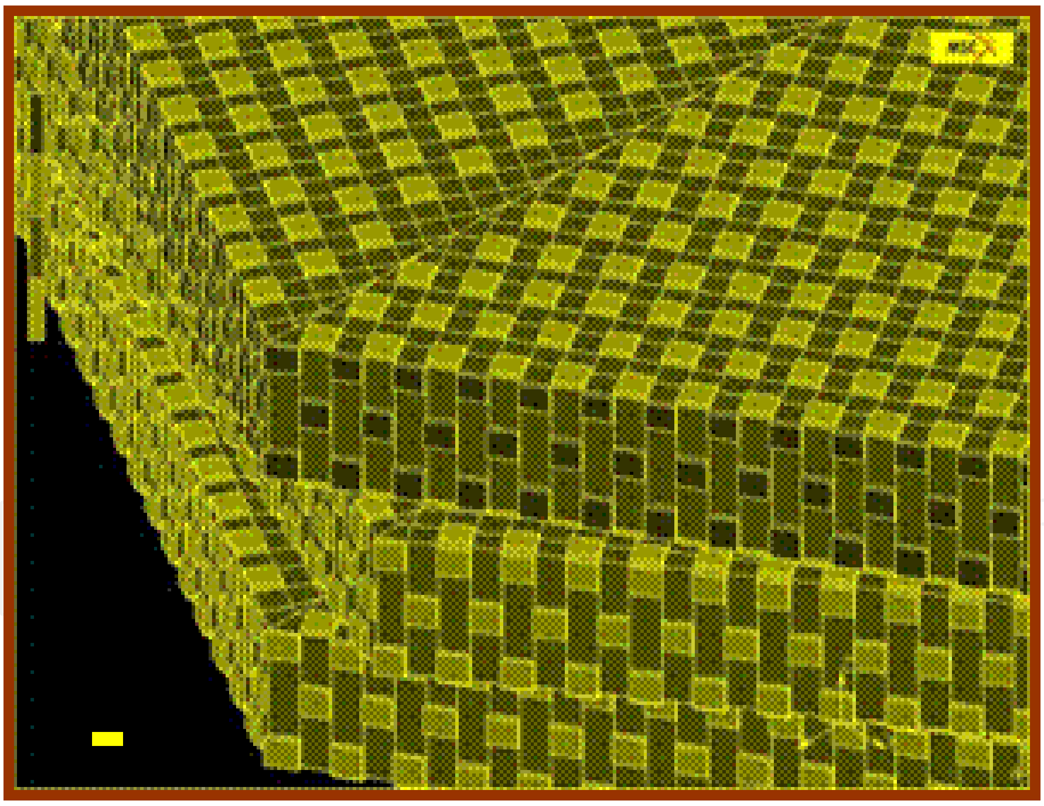

Fig. 6. 3D FE model of nacre with nanoasperities (Katti et al. 2004).

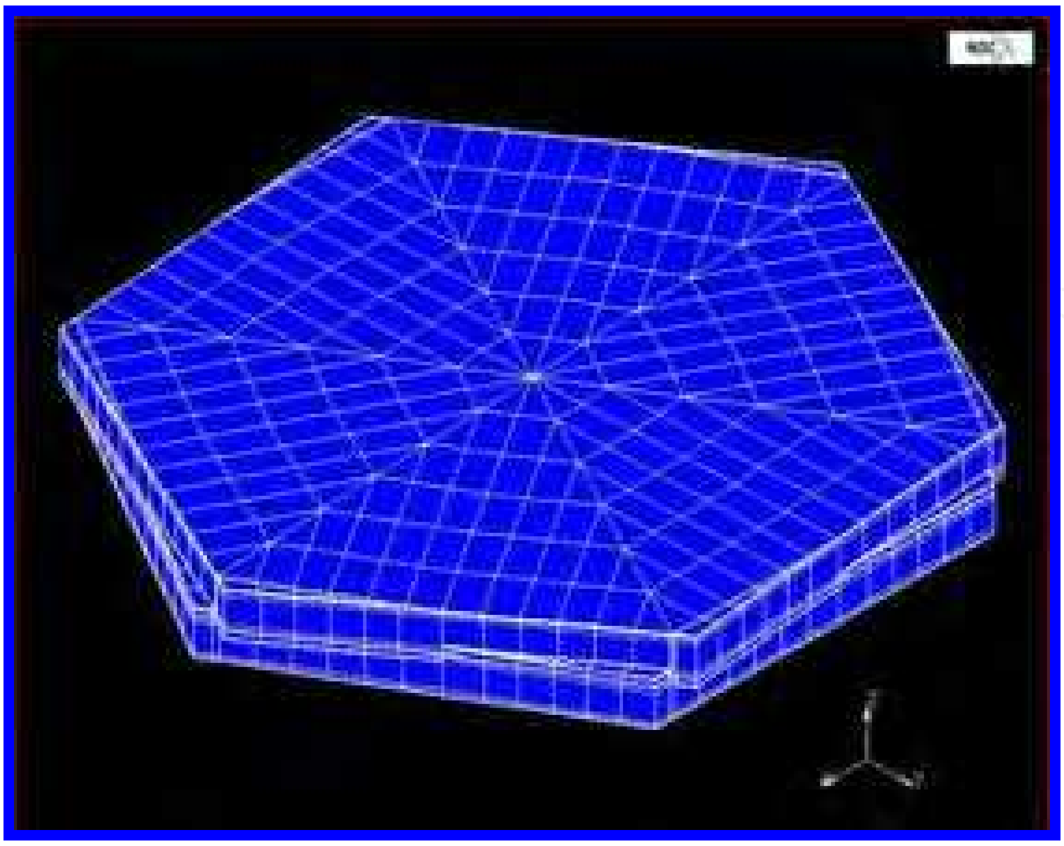

Fig. 7. 3D FE model of nacre with platelet interlocks (Katti et al. 2005).

Li et al. (Li et al. 2004) used microindentation and AFM imaging techniques to study the deformation behavior of nacre. They observed plastic deformation in the aragonite platelets around the crack tip which indicated that the aragonite platelets are not brittle in nature but somewhat ductile. The plastic deformation allows the material to redistribute stress around strain concentrated site, thereby eliminating stress concentration that results in blunting the crack tip. They believed that the ductility of aragonite platelets results from a large number of nanograins which are the basic building blocks. They suggested that the deformability of aragonite platelets along with crack deflection, platelet slip, and organic adhesive interlayer result in a unusual increase in toughness of nacre. Bruet et al. (Bruet et al. 2005) investigated deformation in nacre using atomic force microscopy (AFM) and nanoindentation. They performed nanoindentation tests on nacre and observed the deformation of the indented region using AFM. AFM images showed flattening of the nanoasperities, plastic deformation, pileup around indent and no microcracks in the pileup region. Deformation at nanoscale revealed ductile behavior of aragonite platelets that is not expected to be present in case of a ceramic which is expected to exhibit microcracking under the tensile stresses observed in the pileup region and fail in a brittle manner. The observed ductility might be due to the small length scale or may indicate that the obstructed organic molecules within the platelet lessen any defects and impart ductility to the deformation process. The pileup zones around the indents indicated the ability of nanoasperities to undergo plastic deformation to accommodate strain caused by the indenter tip. Bruet et al. suggested that plastic deformation of the nanoasperities may occur initially and can act as a safety mechanism prior to the intertablet shear. Barthelat et al. (Barthelat et al. 2006, Barthelat and Espinosa 2007) investigated the mechanical performance of nacre using experiments and finite element modeling. They suggested that the observed ductility is because of the small length scale, and the nanoasperities and nanograins are not likely to be the key microstructural features controlling the unique mechanical response of nacre (Barthelat et al. 2006). From this experimental study, it was suggested that the viscoplastic energy dissipation in the proteins and other biopolymers present between the platelets associated with the sliding of the platelets in nacre, is a significant fracture toughening mechanism.

Kattis and co-workers (Mohanty et al. 2006) investigated the dynamic nanomechanical response of nacre using dynamic nanoindentation, AFM and Fourier transform infrared spectroscopy (FTIR). Dynamic nanoindentation tests were performed at different loads with varying frequency. Loss modulus (E'') and tan δ values were observed to increase with increase in testing frequency. Their observation of results at lower indentation depths indicated that the mineral phase exhibits viscoelastic behavior which is not expected in case of a ceramic material. Viscoelastic nature of the aragonite platelets was attributed to the presence of nanograins and water within the platelets. Kattis and co-workers (Verma et al. 2007) further utilized 2D-FTIR spectroscopy and deconvolution analysis to describe the nature and location of water present in nacre. Later, Li et al. (Li, Xu and Wang 2006) observed nanograin rotation and deformation while pulling nacre samples in tension by in situ AFM imaging. They suggested that the nanograins are closely packed by the biopolymer adhesive to form a robust structure. When nacre is pulled in tension, the biopolymer between the nanograins is stretched that allows enough space for some nanograins to rotate. During rotation, these nanograins push neighboring nanograins and also undergo deformation. They suggested that the grain rotation and deformation results in high deformability of the aragonite platelets and are two key mechanisms for energy dissipation in nacre. Meyers et al. (Meyers et al. 2008) investigated the role of organic layer on the mechanical strength of nacre. They concluded that the primary role of the organic layer is to subdivide the $CaCO_3$ matrix into platelets with thickness of 0.5 μm. It was also suggested that the scale of the structural components in nacre is an important parameter. Mohanty et al. (Mohanty, Katti and Katti 2008) investigated the mechanics of mineral-protein interface of nacre using force mode AFM. Protein molecules were pulled from the cleaved nacre surface using AFM and the force required to pull the protein molecules was measured. Results indicated that the protein molecules withstand a large force (~6 nN), before they are pulled off of the aragonite platelet. These forces are several orders of magnitude higher than those obtained for unfolding of domains in a single protein molecule. They estimated the force of adhesion between the organic phase and the aragonite platelet for the first time. They suggested that the large work of adhesion can lead to a large amount of energy dissipation by the protein molecules and contribute towards the bulk toughness of nacre. This indicates a significant role of organic-inorganic interactions on the mechanical response of nacre.

Some researchers have used micromechanical modeling to predict the mechanical behavior of nacre (Zuo and Wei 2008, Bertoldi, Bigoni and Drugan 2008). Zuo and Wei (Zuo and Wei 2008) suggested that the deformation in nacre can be well described by modified shear-lag model considering the elastic-plastic hardening property of the protein. Tushtev et al. (Tushtev, Murck and Grathwohl 2008) showed using finite element simulations that the high stiffness of nacre under tensile load in longitudinal direction is only possible, if the organic layer is incompressible. They pointed that the organic layer plays a key role on the load transfer between the platelets which affects the stiffness of nacre. Sumitomo et al. (Sumitomo et al. 2008a, Sumitomo et al. 2008b) used transmission electron microscopy to observe the nanoscale deformation structures in nacre. They observed strong adhesion of organic phase to the mineral plates and high ductile behavior of the organic matrix (Sumitomo et al. 2008a). Viscoelastic reformation of the matrix ligaments after failure was also observed. Nanograin separation, nanograin shear, and crack bridging due to organic matrix ligament formation within the fractured platelets were observed. They suggested that toughening of nacre occurs in a hierarchical manner from nano to macroscale; i.e. from nanograins, to platelets and to bulk nacre.

As discussed in this section, various different mechanisms have been proposed in literature those contribute towards the energy dissipation in nacre. These mechanisms are summarized below:
Crack diversion and crack branching make crack propagation very tortuous.
Crack bridging by the ligaments of organic matrix.
Formation of microcracks.
Frictional resistance due to presence of nanoasperities and mineral bridges have marginal effect on the toughness of nacre.
Unfolding of protein domains and breaking of crosslinks in the organic phase.
Plasticizing effect of water present in nacre.
Platelet interlocks.
Viscoelastic behavior of the organic phase.
Viscoelastic behavior of the mineral platelets.
Rotation and deformation of nanograins.

3. Biomimicking Efforts

Highly organized microarchitecture and extraordinary mechanical response of nacre have inspired scientists to develop synthetic nanocomposite materials mimicking nacre. Till date, several attempts have been made using various reienforcing materials and different processing methods to develop layered nanocomposite materials those mimic the structure of nacre (Sellinger et al. 1998, Almqvist et al. 1999, Feng et al. 2000, Tang et al. 2003, Zhang et al. 2002, Zhang et al. 2004, Zhang et al. 2006, Gehrke et al. 2005, Bennadji-Gridi, Smith and Bonnet 2006, Wei et al. 2007, Long et al. 2007, Chen et al. 2008, Podsiadlo et al. 2007, Podsiadlo et al. 2008, Lin et al. 2008). Sellinger et al. (Sellinger et al. 1998) synthesized poly (dodecylmethacrylae)/silica nanocomposite using a self assembly process based on a simple dip-coating procedure. They started with a solution of silica, surfactant and organic monomers, formation of micelles and partitioning of the organic constituents into micellar interiors occurred due to evaporation during dip-coating. Organic and inorganic precursors get organized into the desired nanolaminated form with subsequent self-assembly silica-surfactant-monomer micellar species. Finally, the nanocomposite assembly process is completed with polymerization that fixes the structure. Almqvist et al. (Almqvist et al. 1999) fabricated laminated nanocomposite materials using talc tablets as the inorganic phase and polyvinylacetate as the organic phase and investigated seven different physical fabrication methods. In this work 10 wt% of organic was used as it was difficult to wet the talc tablets with an organic content of 5 wt%. It was suggested that align of tablets can be obtained by using a suitable processing method. No significant improvement in the mechanical properties was observed due to improvement in tablet orientation. Feng et al. (Feng et al. 2000) synthesized alumina/aramid fiber reinforced epoxy composites containing five alumina (0.38 m thick) lamnas and four aramid fiber reinforced epoxy strips (0.18 mm thick) alternatively. The synthesized composite exhibited a work of fracture that is 80 times of that of monolithic alumina. Tang et al. (Tang et al. 2003) prepared a nanostructured composite with alternating organic and inorganic layers mimicking nacre by sequential deposition of polelectrolytes [poly(diallydimethylammonium) chloride polycation] and clays. The saw-tooth pattern in the stretching curves revealed gradual breakage of ionic crosslinks in polyelectrolyte chains which is similar to the unfolding of protein domains in nacre. The tensile strength of these multilayered composites was comparable to that of nacre. Zhang et al. (Zhang et al. 2004) synthesized silica/poly(methacryloxyethyl hexadecyldimethyl ammonium bromide) nanocomposite thin films by supermolecular self-assembly method on glass substrate. It was confirmed that the nanocomposite films resemble the laminated structure in nacre. Zhang et al. (Zhang et al. 2006) prepared poly(tripropylene glycol diacrylate) (i.e. poly-TPGDA)/indium-tin-oxide (ITO) nanocomposite films by dip-coating method where the self-assembly was induced by evaporation. Results indicated that the films have organic and inorganic layers with orderly arrangement. Gehrke et al. (Gehrke et al. 2005) used a unique method to synthesize artificial nacre remineralization of the insoluble matrix of natural nacre. Prior to this, nacre was demineralized and the soluble proteins were removed. Scanning electron microscope images of the fractured surface showed that the artificial nacre closely resembles the natural nacre. Bennadji-Gridi et al. (Bennadji-Gridi et al. 2006) prepared nacre-like films based on Na/Ca montmorillonite by drying the dispersions with low concentrations of delaminated platelets. A dense brick-like structure was obtained after complete drying using a sodium salt as deflocculant. The observed mechanical properties were not comparable to that of nacre. Wei et al. (Wei et al. 2007)designed a structure mimicking nacre by alternating layer-by-layer deposition of polymer films and $CaCO_3$ strata. The organic matrix composed of layer-by-layer polymer thin films of diazo-resins (DAR) and poly (acrylic acid) (PAA). The role of DAR is to cross-link the thin films and PAA provides a surface for facilitating the biomineralization. The inorganic layers of CaCO3 strata were prepared via CO2 diffusion method. The thickness of inorganic layer can be controlled by varying the diffusion time of CO2 and the thickness of organic matrix can be controlled by the number of polymer thin film layers. Long et al. (Long et al. 2007) prepared polyacrylamide-clay nacre-like nanocomposites by electrophoretic deposition of montmorillonite modified by acrylamide monomers in an aqueous suspension. Electrophoretic deposition was carried out using the suspension of organic clay in distilled water. Then the deposit on the electrode was polymerized under ultraviolet radiation using a photo-initiator. The nanocomposite was observed to possess a uniform and organized layer-by-layer structure which was similar to the brick-and-mortar structure of natural nacre. These nacre-like composites exhibited significant improvement in elastic modulus and hardness values as compared to that of pure montmorillonite. Chen et al. (Chen et al. 2008) fabricated inorganic/organic nanocomposites using clay nano-platelets as the mineral and polyimide as the organic constituent. An ordered nanostructure with alternating organic and inorganic layers was achieved using a centrifugal deposition process. Improvement in mechanical properties was observed, but they were not comparable to that of nacre. Podsiadlo et al. (Podsiadlo et al. 2007) prepared a high-strength nanocomposite by sequential deposition using clay and L-3,4-Dihydroxyphenylalanine (DOPA) polymer which is an amino acid present in mussel protein. DOPA was used as it is known to have high affinity for a variety of chemically distinct surfaces: organic and inorganic, via coordination, covalent and hydrogen bonds. Significant improvement in ultimate tensile strength was observed with the addition of DOPA. In another study, Podsiadlo et al. (Podsiadlo et al. 2008) prepared nacre-like structures by using poly(vinyl alcohol) (PVA) and Na-montmorillonite clay nanosheets. They undertook a layer-by-layer assembly technique. Further, PVA and montmorillonite were bound mainly through weak hydrogen bonds and PVA was crosslinked using metal cations after assembly, to introduce ionic bonds in the structure. A double network of sacrificial bonds is created with the introduction of ionic bonds. During deformation, it is expected These sacrificial cross-links can break and form again in the course of deformation. The mechanical property of these composites exhibited significant improvement. The cross-linked films exhibited an ultimate tensile strength (~ 320 ± 40 MPa) which is more than twice as high as that of nacre (~ 80 – 135 MPa). Lin et al. (Lin et al. 2008) introduced a special assemble method using hydrothermal-electrophoretic techniques to prepare clay based nanocomposites that mimics nacre, both in structure and composition. In the first step, the polymer is intercalated into the interlayer space of montmorillonite by hydrothermal process and electrophoretic deposition is carried out in the second step. Results showed an increase in elastic modulus value as compared to that of pure montmorillonite. As discussed in this section, several attempts have been made to mimic the structure of nacre till date. None of the composites have exhibited an improvement in toughness as in case of nacre. One possible reason might be that all these composites do not possess the interlocking features observed in nacre. Moreover, the organic phase in case of nacre exhibits a very high elastic modulus.

4. Multiscale Modeling

Nacre is a nanocomposite that has a hierarchical microstrcture and exhibits unique mechanical properties. There are several structural details at various length scales which influence the overall mechanical response of nacre. Modeling mechanical behavior of nacre through models is necessary to understand the role of structure at different length scales on overall mechanical behavior. Traditional routes of modelling composites such as those based on micromechanics and continuum theories are not applicable or practical over the large length scale (nm to mm) and time scale (fs to s) and requires unique multiscale methodologies. Kattis and co-workers have used different modeling tools along with experiments to investigate the mechanical response of nacre at different length scales based on a unique hierarchical multiscale modelling methodology (Ghosh et al. 2007, Ghosh et al. 2008, Katti et al. 2001, Katti and Katti 2001, Katti et al. 2004, Katti et al. 2005, Katti, Mohanty and Katti 2006, Katti and Katti 2006, Mohanty et al. 2006, Mohanty et al. 2008, Verma et al. 2006, Verma et al. 2007). They have quantitatively described the role of each of nanostructural details on the mechanics and deformation behavior of nacre. The identified key mechanisms influencing the overall mechanical behaviour of nacre have been quantitatively identified. Katti et al. have extensively used finite element (FE) modeling to understand the mechanical response of nacre. 3D finite element models of nacre were constructed based on interlocked brick and mortar architecture. Material properties of the constituents were included in the model. Elastic modulus of aragonite was obtained from nanoindentation tests to include in the model. Mechanical properties of organic were not available at the time of study and were predicted from finite element simulations applying tensile and compressive stresses to the model. Mineral bridges and nanoscale asperities were incorporated in the finite element models. The size, shape and distribution of these features were included according to the reported observations found in literature. Interlocks were constructed by rotating the stack of two aragonite platelets by five degrees relative to each other and then protruding the upper platelet into the lower platelet through a distance of 50 nm. This penetration distance of 50 nm was obtained from the SEM images which include the 20 nm thick organic film between two aragonite platelets. Simulations results indicated a very high elastic modulus value for the organic phase. FE simulation results revealed that the presence of mineral bridges and nanoasperities in the nacre structure have marginal effect on the mechanical response of nacre. The obtained stress-strain response of nacre from FE simulation with interlocks indicated that the observed deformations in nacre are results of deformation of the organic phase, inorganic phase and failure of the interlocks. The progressive failure of the platelet interlocks contribute to the high toughness and strength of nacre.

MD simulations have also been performed to understand role of molecular interactions on the mechanical behavior of nacre. Results showed that the mineral significantly influences the mechanical response of the organic phase. Protein molecules were pulled experimentally from the cleaved nacre surface using force mode atomic force microscopy. Experimental results were in agreement with the MD simulation results which indicated that a high force is required to pull the protein molecules. These simulation and experimental studies led to some important findings that help better understand the underlying mechanisms responsible for the unique mechanical response of nacre. Based on these studies, Katti et al. have identified the key components that contribute towards the high strength and toughness of nacre as given below:
Unique properties of the organic phase in the confined space between the platelets.
Size and shape of platelets (i.e. structure at micro scale).
Interlocking aragonite platelets.
Bonded and non-bonded molecular interactions at the organic-inorganic interface.

5. Conclusions

In summary, here we present the unique aspects of the details of the structure of nacre, the inner layer of many molluscan seashells. Also described is the state-of-art in understanding the structure-property relationships in nacre covering the length span from nanoscale features to a length scale of mm. It appears that this unique architecture of nacre and its resulting exceptional properties of fracture toughness and strength have intrigued materials scientists over decades and has been a subject of biomimetic design for over 4 decades. We also present recent attempts to mimic structure and mimic properties using engineered systems. It appears that engineering routes suffer from the inherent incapability of achieving hierarchy although details at any given length scale are easily achieved. This hierarchy itself is of paramount importance that gives properties such as toughness and structural redundancy to biological materials and structures. Unearthing the key to mechanisms of hierarchy (which are most definitely biological) needs to be the fundamental goal of the field of biomimetics which if successful has far reaching applications in defence, structures, medicine and other areas. Unearthing details of structure in nacre has been extensively investigated but unearthing the mechanisms by which biology accomplishes hierarchy has not been sufficiently investigated. None the less, nature continues to both inspire and intrigue and we continue to be inspired to design and duplicate details copied from nature intrigued by its simple processing routes and engineering.

6. References

Abelson, P. H. (1954) Organic constituents of fossils. *Carnegie Inst. Washington Yearb,* 53**,** 97-101.

Addadi, L., J. Moradian, E. Shay, N. G. Maroudas & S. Weiner (1987) A CHEMICAL-MODEL FOR THE COOPERATION OF SULFATES AND CARBOXYLATES IN CALCITE CRYSTAL NUCLEATION - RELEVANCE TO BIOMINERALIZATION. *Proceedings of the National Academy of Sciences of the United States of America,* 84**,** 2732-2736.

Addadi, L. & S. Weiner (1985) INTERACTIONS BETWEEN ACIDIC PROTEINS AND CRYSTALS - STEREOCHEMICAL REQUIREMENTS IN BIOMINERALIZATION. *Proceedings of the National Academy of Sciences of the United States of America,* 82**,** 4110-4114.

Addadi, L. & S. Weiner (1997) Biomineralization - A pavement of pearl. *Nature,* 389**,** 912-&.

Almqvist, N., N. H. Thomson, B. L. Smith, G. D. Stucky, D. E. Morse & P. K. Hansma (1999) Methods for fabricating and characterizing a new generation of biomimetic materials. *Materials Science & Engineering C-Biomimetic and Supramolecular Systems,* 7**,** 37-43.

Barthelat, F. & H. D. Espinosa (2007) An experimental investigation of deformation and fracture of nacre-mother of pearl. *Experimental Mechanics,* 47**,** 311-324.

Barthelat, F., C. M. Li, C. Comi & H. D. Espinosa (2006) Mechanical properties of nacre constituents and their impact on mechanical performance. *Journal of Materials Research,* 21**,** 1977-1986.

Belcher, A. M., X. H. Wu, R. J. Christensen, P. K. Hansma, G. D. Stucky & D. E. Morse (1996) Control of crystal phase switching and orientation by soluble mollusc-shell proteins. *Nature,* 381**,** 56-58.

Bennadji-Gridi, F., A. Smith & J. P. Bonnet (2006) Montmorillonite based artificial nacre prepared via a drying process. *Materials Science and Engineering B-Solid State Materials for Advanced Technology,* 130**,** 132-136.

Bertoldi, K., D. Bigoni & W. J. Drugan (2008) Nacre: An orthotropic and bimodular elastic material. *Composites Science and Technology,* 68**,** 1363-1375.

Boggild, O. B. (1930) The shell structure of the mollusks. *K. danske Vidensk. Selsk. Skr.,* 2**,** 232-325.

Bruet, B. J. F., H. J. Qi, M. C. Boyce, R. Panas, K. Tai, L. Frick & C. Ortiz (2005) Nanoscale morphology and indentation of individual nacre tablets from the gastropod mollusc Trochus niloticus. *Journal of Materials Research,* 20**,** 2400-2419.

Chen, R. F., C. A. Wang, Y. Huang & H. R. Le (2008) An efficient biomimetic process for fabrication of artificial nacre with ordered-nano structure. *Materials Science & Engineering C-Biomimetic and Supramolecular Systems,* 28**,** 218-222.

Currey, J. D. (1976) Further studies on the mechanical properties of mollusc shell material. *J. Zool. Lond.,* 180**,** 445-453.

Currey, J. D. (1977) MECHANICAL-PROPERTIES OF MOTHER OF PEARL IN TENSION. *Proceedings of the Royal Society of London Series B-Biological Sciences,* 196**,** 443-&.

Currey, J. D. 1980. *The Mechanical Properties of Biological Materials*. London, UK: Cambridge University Press.

Currey, J. D. & J. D. Taylor (1974) The mechanical behavior of some molluscan hard tissues. *J. Zool. Lond.,* 173**,** 395-406.

Erben, H. K. (1972) On the structure and growth of the nacreous tablets in gastropods. *Biomineralisation,* 4.

Evans, A. G., Z. Suo, R. Z. Wang, I. A. Aksay, M. Y. He & J. W. Hutchinson (2001) Model for the robust mechanical behavior of nacre. *Journal of Materials Research,* 16**,** 2475-2484.

Feng, Q. L., F. Z. Cui, G. Pu, R. Z. Wang & H. D. Li. 2000. Crystal orientation, toughening mechanisms and a mimic of nacre. 19-25.

Fritz, M., A. M. Belcher, M. Radmacher, D. A. Walters, P. K. Hansma, G. D. Stucky, D. E. Morse & S. Mann (1994) Flat pearls from biofabrication of organized composites on inorganic substrates. *Nature,* 371**,** 49-51.

Gehrke, N., N. Nassif, N. Pinna, M. Antonietti, H. S. Gupta & H. Colfen (2005) Retrosynthesis of nacre via amorphous precursor particles. *Chemistry of Materials,* 17**,** 6514-6516.

Ghosh, P., D. R. Katti & K. S. Katti (2007) Mineral proximity influences mechanical response of proteins in biological mineral-protein hybrid systems. *Biomacromolecules,* 8**,** 851-856.

Ghosh, P., D. R. Katti & K. S. Katti (2008) Mineral and protein-bound water and latching action control mechanical behavior at protein-mineral interfaces in biological nanocomposites. *Journal of Nanomaterials*.

Gilbert, P., R. A. Metzler, D. Zhou, A. Scholl, A. Doran, A. Young, M. Kunz, N. Tamura & S. N. Coppersmith (2008) Gradual Ordering in Red Abalone Nacre. *Journal of the American Chemical Society,* 130**,** 17519-17527.

Heuer, A. H., D. J. Fink, V. J. Laraia, J. L. Arias, P. D. Calvert, K. Kendall, G. L. Messing, J. Blackwell, P. C. Rieke, D. H. Thompson, A. P. Wheeler, A. Veis & A. I. Caplan (1992) INNOVATIVE MATERIALS PROCESSING STRATEGIES - A BIOMIMETIC APPROACH. *Science,* 255**,** 1098-1105.

Jackson, A. P., J. F. V. Vincent, D. Briggs, R. A. Crick, S. F. Davies, M. J. Hearn & R. M. Turner (1986) APPLICATION OF SURFACE ANALYTICAL TECHNIQUES TO THE STUDY OF FRACTURE SURFACES OF MOTHER-OF-PEARL. *Journal of Materials Science Letters,* 5**,** 975-978.

Jackson, A. P., J. F. V. Vincent & R. M. Turner (1988) THE MECHANICAL DESIGN OF NACRE. *Proceedings of the Royal Society of London Series B-Biological Sciences,* 234**,** 415-&.

Jackson, A. P., J. F. V. Vincent & R. M. Turner (1989) A PHYSICAL MODEL OF NACRE. *Composites Science and Technology,* 36**,** 255-266.

Jackson, A. P., J. F. V. Vincent & R. M. Turner (1990) COMPARISON OF NACRE WITH OTHER CERAMIC COMPOSITES. *Journal of Materials Science,* 25**,** 3173-3178.

Kamat, S., X. Su, R. Ballarini & A. H. Heuer (2000) Structural basis for the fracture toughness of the shell of the conch Strombus gigas. *Nature,* 405**,** 1036-1040.

Katti, D. R. & K. S. Katti (2001) Modeling microarchitecture and mechanical behavior of nacre using 3D finite element techniques - Part I - Elastic properties. *Journal of Materials Science,* 36**,** 1411-1417.

Katti, D. R., K. S. Katti, J. M. Sopp & M. Sarikaya. 2001. 3D finite element modeling of mechanical response in nacre-based hybrid nanocomposites. 397-404.

Katti, D. R., S. M. Pradhan & K. S. Katti (2004) Modeling the organic-inorganic interfacial nanoasperities in a model bio-nanocomposite, nacre. *Reviews on Advanced Materials Science,* 6**,** 162-168.

Katti, K. S. & D. R. Katti. 2006. Why is nacre so tough and strong? , 1317-1324.

Katti, K. S., D. R. Katti, S. M. Pradhan & A. Bhosle (2005) Platelet interlocks are the key to toughness and strength in nacre. *Journal of Materials Research,* 20**,** 1097-1100.

Katti, K. S., B. Mohanty & D. R. Katti (2006) Nanomechanical properties of nacre. *Journal of Materials Research,* 21**,** 1237-1242.

Kotha, S. P., Y. Li & N. Guzelsu (2001) Micromechanical model of nacre tested in tension. *Journal of Materials Science,* 36**,** 2001-2007.

Li, X., W. C. Chang, Y. J. Chao, R. Wang & M. Chang (2004) Nanoscale Structural and Mechanical Characterization of a Natural Nanocomposite Material: The Shell of Red Abalone. *Nanoletters,* 4**,** 613-617.

Li, X. D., Z. H. Xu & R. Z. Wang (2006) In situ observation of nanograin rotation and deformation in nacre. *Nano Letters,* 6**,** 2301-2304.

Lin, W., C. A. Wang, H. L. Le, B. Long & Y. Huang (2008) Special assembly of laminated nanocomposite that mimics nacre. *Materials Science & Engineering C-Biomimetic and Supramolecular Systems,* 28**,** 1031-1037.

Long, B., C. A. Wang, W. Lin, Y. Huang & J. L. Sun (2007) Polyacrylamide-clay nacre-like nanocomposites prepared by electrophoretic deposition. *Composites Science and Technology,* 67**,** 2770-2774.

Menig, R., M. H. Meyers, M. A. Meyers & K. S. Vecchio (2000) Quasi-static and dynamic mechanical response of Haliotis rufescens (abalone) shells. *Acta Materialia,* 48**,** 2383-2398.

Menig, R., M. H. Meyers, M. A. Meyers & K. S. Vecchio (2001) Quasi-static and dynamic mechanical response of Strombus gigas (conch) shells. *Materials Science and Engineering a-Structural Materials Properties Microstructure and Processing,* 297**,** 203-211.

Meyers, M. A., A. Y. M. Lin, P. Y. Chen & J. Muyco (2008) Mechanical strength of abalone nacre: Role of the soft organic layer. *Journal of the Mechanical Behavior of Biomedical Materials,* 1**,** 76-85.

Mohanty, B., K. S. Katti & D. R. Katti (2008) Experimental investigation of nanomechanics of the mineral-protein interface in nacre. *Mechanics Research Communications,* 35**,** 17-23.

Mohanty, B., K. S. Katti, D. R. Katti & D. Verma (2006) Dynamic nanomechanical response of nacre. *Journal of Materials Research,* 21**,** 2045-2051.

Mutvei, H. (1970) Ultrastructure of the mineral and organic components of molluscan nacreous layers. *Biomineralisation,* 2**,** 49-72.

Nudelman, F., B. A. Gotliv, L. Addadi & S. Weiner (2006) Mollusk shell formation: Mapping the distribution of organic matrix components underlying a single aragonitic tablet in nacre. *Journal of Structural Biology,* 153**,** 176-187.

Podsiadlo, P., A. K. Kaushik, B. S. Shim, A. Agarwal, Z. Y. Tang, A. M. Waas, E. M. Arruda & N. A. Kotov (2008) Can Nature's Design be Improved Upon? High Strength, Transparent Nacre-Like Nanocomposites with Double Network of Sacrificial Cross Links. *Journal of Physical Chemistry B,* 112**,** 14359-14363.

Podsiadlo, P., Z. Q. Liu, D. Paterson, P. B. Messersmith & N. A. Kotov (2007) Fusion of seashell nacre and marine bioadhesive analogs: High-strength nanocomposite by layer-by-layer assembly of clay and L-3,4-dihydroxyphenylaianine polymer. *Advanced Materials,* 19**,** 949-+.

Sarikaya, M. (1994) AN INTRODUCTION TO BIOMIMETICS - A STRUCTURAL VIEWPOINT. *Microscopy Research and Technique,* 27**,** 360-375.

Sarikaya, M., K. E. Gunnison, M. Yasrebi, D. L. Milius & I. A. Aksay. 1990. Mechanical properties-microstrsucture relationship in abalone shell. In *Mat. Res. Soc. Symp. Proc.*, 109-116.

Schaffer, T. E., C. IonescuZanetti, R. Proksch, M. Fritz, D. A. Walters, N. Almqvist, C. M. Zaremba, A. M. Belcher, B. L. Smith, G. D. Stucky, D. E. Morse & P. K. Hansma (1997) Does abalone nacre form by heteroepitaxial nucleation or by growth through mineral bridges? *Chemistry of Materials,* 9**,** 1731-1740.

Sellinger, A., P. M. Weiss, A. Nguyen, Y. F. Lu, R. A. Assink, W. L. Gong & C. J. Brinker (1998) Continuous self-assembly of organic-inorganic nanocomposite coatings that mimic nacre. *Nature,* 394**,** 256-260.

Shen, X. Y., A. M. Belcher, P. K. Hansma, G. D. Stucky & D. E. Morse (1997) Molecular cloning and characterization of lustrin A, a matrix protein from shell and pearl nacre of Haliotis rufescens. *Journal of Biological Chemistry,* 272**,** 32472-32481.

Smith, B. L., T. E. Schaffer, M. Viani, J. B. Thompson, N. A. Frederick, J. Kindt, A. Belcher, G. D. Stucky, D. E. Morse & P. K. Hansma (1999) Molecular mechanistic origin of the toughness of natural adhesives, fibres and composites. *Nature,* 399**,** 761-763.

Song, F. & Y. L. Bai (2001) Mineral bridges of nacre and its effects. *Acta Mechanica Sinica,* 17**,** 251-257.

Song, F., A. K. Soh & Y. L. Bai (2003) Structural and mechanical properties of the organic matrix layers of nacre. *Biomaterials,* 24**,** 3623-3631.

Song, F., X. H. Zhang & Y. L. Bai (2002) Microstructure and characteristics in the organic matrix layers of nacre. *Journal of Materials Research,* 17**,** 1567-1570.

Su, X., A. M. Belcher, C. M. Zaremba, D. E. Morse, G. D. Stucky & A. H. Heuer (2002) Structural and microstructural characterization of the growth lines and prismatic microarchitecture in red abalone shell and the microstructures of abalone "Flat pearls". *Chem. Mater.,* 14**,** 3106-3117.

Sumitomo, T., H. Kakisawa, Y. Owaki & Y. Kagawa (2008a) In situ transmission electron microscopy observation of reversible deformation in nacre organic matrix. *Journal of Materials Research,* 23**,** 1466-1471.

Sumitomo, T., H. Kakisawa, Y. Owaki & Y. Kagawa (2008b) Transmission electron microscopy observation of nanoscale deformation structures in nacre. *Journal of Materials Research,* 23**,** 3213-3221.

Tang, Z. Y., N. A. Kotov, S. Magonov & B. Ozturk (2003) Nanostructured artificial nacre. *Nature Materials,* 2**,** 413-U8.

Taylor, J. D. (1973) The structural evolution of the bivalve shell. *Palaeontology,* 16**,** 519-534.

Taylor, J. D., W. J. Kennedy & A. Hall (1969) Shell structure and mineralogy of the Bivalvia: Introduction Nuculacea - Trigonacea. *Bull. Br. Mus. Hist. Zool.,* Suppl. 3, 1-125.

Taylor, J. D., W. J. Kennedy & A. Hall (1973) The shell structure and mineralogy of the Bivalvia: Lucinacea - Clavagellacea, conclusions. *Bull. Br. Mus. nat. Hist.,* 22, 255-294.

Taylor, J. D. & M. Layman (1972) Mechanical properties of bivalve shell structures. *Palaeontology,* 15, 73-87.

Tushtev, K., M. Murck & G. Grathwohl (2008) On the nature of the stiffness of nacre. *Materials Science & Engineering C-Biomimetic and Supramolecular Systems,* 28, 1164-1172.

Verma, D., K. Katti & D. Katti (2006) Photoacoustic FTIR spectroscopic study of undisturbed nacre from red abalone. *Spectrochimica Acta Part a-Molecular and Biomolecular Spectroscopy,* 64, 1051-1057.

Verma, D., K. Katti & D. Katti (2007) Nature of water in nacre: A 2D Fourier transform infrared spectroscopic study. *Spectrochimica Acta Part a-Molecular and Biomolecular Spectroscopy,* 67, 784-788.

Wang, R. Z., Z. Suo, A. G. Evans, N. Yao & I. A. Aksay (2001) Deformation mechanisms in nacre. *Journal of Materials Research,* 16, 2485-2493.

Wang, R. Z., H. B. Wen, F. Z. Cui, H. B. Zhang & H. D. Li (1995) OBSERVATIONS OF DAMAGE MORPHOLOGIES IN NACRE DURING DEFORMATION AND FRACTURE. *Journal of Materials Science,* 30, 2299-2304.

Watabe, N. (1955) The observation of the surface structure of the cultured pearls relating to color and luster. *Rep. Fac. Fish. Pref. Univ. Mie.,* 2, 18-26.

Wei, H., N. Ma, F. Shi, Z. Q. Wang & X. Zhang (2007) Artificial nacre by alternating preparation of layer-by-layer polymer films and CaCO3 strata. *Chemistry of Materials,* 19, 1974-1978.

Weiner, S. (1979) ASPARTIC ACID-RICH PROTEINS - MAJOR COMPONENTS OF THE SOLUBLE ORGANIC MATRIX OF MOLLUSK SHELLS. *Calcified Tissue International,* 29, 163-167.

Weiner, S. (1983) MOLLUSK SHELL FORMATION - ISOLATION OF 2 ORGANIC MATRIX PROTEINS ASSOCIATED WITH CALCITE DEPOSITION IN THE BIVALVE MYTILUS-CALIFORNIANUS. *Biochemistry,* 22, 4139-4145.

Weiner, S. (1984) ORGANIZATION OF ORGANIC MATRIX COMPONENTS IN MINERALIZED TISSUES. *American Zoologist,* 24, 945-951.

Weiner, S., H. A. Lowenstam, B. Taborek & L. Hood (1979) FOSSIL MOLLUSK SHELL ORGANIC MATRIX COMPONENTS PRESERVED FOR 80 MILLION YEARS. *Paleobiology,* 5, 144-150.

Weiner, S., Y. Talmon & W. Traub (1983) ELECTRON-DIFFRACTION OF MOLLUSK SHELL ORGANIC MATRICES AND THEIR RELATIONSHIP TO THE MINERAL PHASE. *International Journal of Biological Macromolecules,* 5, 325-328.

Weiner, S. & W. Traub (1980) X-RAY-DIFFRACTION STUDY OF THE INSOLUBLE ORGANIC MATRIX OF MOLLUSK SHELLS. *Febs Letters,* 111, 311-316.

Weiner, S. & W. Traub (1981) STRUCTURE OF ORGANIC MATRICES IN MOLLUSK SHELLS - EVIDENCE FOR EPITAXIAL-GROWTH IN BIOMINERALIZATION. *Journal of Rheumatology,* 8, 1011-1012.

Weiner, S. & W. Traub (1984) MACROMOLECULES IN MOLLUSK SHELLS AND THEIR FUNCTIONS IN BIOMINERALIZATION. *Philosophical Transactions of the Royal Society of London Series B-Biological Sciences,* 304, 425-&.

Wise, S. W. & Devillie.J (1971) SCANNING ELECTRON MICROSCOPY OF MOLLUSCAN SHELL ULTRASTUCTURES - SCREW DISLOCATIONS IN PELECYPOD NACRE. *Transactions of the American Microscopical Society,* 90**,** 376-&.

Yao, N., A. Epstein & A. Akey (2006) Crystal growth via spiral motion in abalone shell nacre. *Journal of Materials Research,* 21**,** 1939-1946.

Zaremba, C. M., A. M. Belcher, M. Fritz, Y. L. Li, S. Mann, P. K. Hansma, D. E. Morse, J. S. Speck & G. D. Stucky (1996) Critical transitions in the biofabrication of abalone shells and flat pearls. *Chemistry of Materials,* 8**,** 679-690.

Zaremba, C. M., A. M. Belcher, M. Fritz, D. E. Morse, J. S. Speck, P. K. Hansma & G. D. Stucky (1995) ORGANIC-INORGANIC INTERFACES IN THE ULTRASTRUCTURE OF RED ABALONE NACRE. *Abstracts of Papers of the American Chemical Society,* 209**,** 584-INOR.

Zhang, S. M., Y. J. Gao, Z. J. Zhang, H. X. Dang, W. M. Liu & Q. J. Xue (2002) Preparation and characterization of self-assembly nanocomposite thin film mimicking nacre. *Acta Physico-Chimica Sinica,* 18**,** 451-454.

Zhang, S. M., J. W. Zhang, Z. J. Zhang, H. X. Dang, W. M. Liu & Q. J. Xue (2004) Preparation and characterization of self-assembled organic-inorganic nacre-like nanocomposite thin films. *Materials Letters,* 58**,** 2266-2269.

Zhang, X., C. L. Liu, W. J. Wu & J. F. Wang (2006) Evaporation-induced self-assembly of organic-inorganic ordered nanocomposite thin films that mimic nacre. *Materials Letters,* 60**,** 2086-2089.

Zuo, S. C. & Y. G. Wei (2008) Microstructure observation and mechanical behavior modeling for limnetic nacre. *Acta Mechanica Sinica,* 24**,** 83-89.

Biomimetics Learning from Nature

Edited by Amitava Mukherjee

ISBN 978-953-307-025-4
Hard cover, 534 pages
Publisher InTech

Published in print edition March, 2010

Nature's evolution has led to the introduction of highly efficient biological mechanisms. Imitating these mechanisms offers an enormous potential for the improvement of our day to day life. Ideally, by bio-inspiration we can get a better view of nature's capability while studying its models and adapting it for our benefit. This book takes us into the interesting world of biomimetics and describes various arenas where the technology is applied. The 25 chapters covered in this book disclose recent advances and new ideas in promoting the mechanism and applications of biomimetics.

Kalpana S. Katti, Dinesh R. Katti and Bedabibhas Mohanty (2010). Biomimetic Lessons Learnt from Nacre, Biomimetics Learning from Nature, Amitava Mukherjee (Ed.), ISBN: 978-953-307-025-4, InTech, Available from: http://www.intechopen.com/books/biomimetics-learning-from-nature/biomimetic-lessons-learnt-from-nacre

INTECH
open science | open minds

InTech Europe
University Campus STeP Ri
Slavka Krautzeka 83/A
51000 Rijeka, Croatia
Phone: +385 (51) 770 447
Fax: +385 (51) 686 166
www.intechopen.com

InTech China
Unit 405, Office Block, Hotel Equatorial Shanghai
No.65, Yan An Road (West), Shanghai, 200040, China
中国上海市延安西路65号上海国际贵都大饭店办公楼405单元
Phone: +86-21-62489820
Fax: +86-21-62489821